Co-Ligand Involvement in Ground and Excited States of Electron-Rich (Polypyridyl)Pt^{II} Complexes

Axel Klein,*[a] Joris van Slageren,*[b][‡] and Stanislav Záliš[c]

Keywords: Emission / Platinum / N ligands / Photophysics / Optical spectroscopy / Theoretical calculations / DFT / Crystal structure

The electronic absorption and luminescence properties of electron-rich organometallic platinum(II) complexes with aromatic α-diimine ligands [(α-diimine)PtR$_2$] (R = alkyl, alkynyl, Ph or Mes, Mes = 2,4,6-trimethylphenyl) were examined. The crystal and molecular structures of [(bpy)PtMe$_2$], [(tap)PtPh$_2$] and [(tmphen)PtMes$_2$] were determined from single-crystal XRD and discussed in view of intermolecular interactions that influence the emission behaviour. The combination of theoretical calculations (DFT) and spectroscopic techniques (absorption and emission) revealed the character of electronic transitions and excited states. In particular they showed that the co-ligand involvement in the frontier orbitals is small for R = Me, but large in case of R = alkynyl, Ph or Mes. Depending on the chelate ligand and its substitution pattern, the emission efficiencies of the complexes cover a wide range from strong emission in fluid solution at ambient temperature to very weak emission in rigid matrices (glasses) at low temperatures with no emission at ambient temperature. The emission lifetimes, determined at low temperature in solvent glasses, mainly depend on the chelate ligand and not on the co-ligands. The emission quantum yields of the complexes in solution at room temperatures are much larger for R = Mes than for R = Ph or Me. The emission bands for the complexes with unsaturated co-ligands show slight structuring at low temperatures in contrast to the alkyl-substituted ones.

Introduction

Platinum(II) complexes with α-diimine ligands and their photophysical properties have been the subject of much interest in the last three decades.[1−21] Their square-planar geometry provides the possibility to introduce selectively properly designed α-diimine ligands and suitable co-ligands in a coplanar arrangement and thus allows the tailoring of molecules for potential application as photosensitizers or photocatalysts.[16,22−24] The platinum centre itself provides relatively high stability against isomerisation or thermal decomposition. Electronic transitions in such complexes span a broad range depending on both the diimine ligand and the co-ligand(s) (see Scheme 1). Ligand field (LF or d−d) transitions occur as the lowest transition in case where the diimine ligand is a weak acceptor and the co-ligand is a relatively weak σ donor. When choosing the z axis coincident with the main symmetry axis (in C_{2v} symmetry), the highest occupied MOs are $d_{x^2-y^2}$ or d_{z^2}, while d_{yz} is the LUMO (Scheme 1, case A). In this case metal-to-ligand charge transfer (MLCT) transitions lie at higher energies. Examples of this situation are [(bpy)PtX$_2$] (X = Cl, Br, I).[6,8,11,18] If the π and π* orbitals of the diimine ligand are higher and lower in energy than the filled and empty d(Pt) orbitals, respectively, the lowest-energy electronic transitions are of intraligand (π-π*) character (Scheme 1, B). This situation was found for [(bpy)Pt(en)]$^{2+}$,[11] and is caused by the stronger ligand field of the en ligand compared to X. If the diimine ligand is a good π acceptor, its

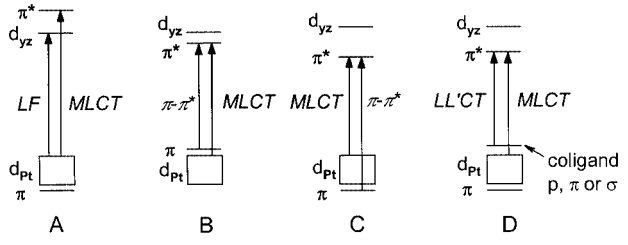

Scheme 1. Qualitative MO scheme for (diimine)platinum complexes assuming C_{2v} symmetry; note that the z axis coincides with the (main) C_2 axis and the x axis is perpendicular to the coordination plane

[a] Institut für Anorganische Chemie, Universität Stuttgart, Pfaffenwaldring 55, 70569 Stuttgart, Germany
E-mail: aklein@iac.uni-stuttgart.de
[b] Institute of Molecular Chemistry, Universiteit van Amsterdam, Nieuwe Achtergracht 166, 1018 WV Amsterdam, The Netherlands
[c] J. Heyrovský Institute of Physical Chemistry, Academy of Sciences of the Czech Republic, Dolejškova 3, 18000 Prague 8, Czech Republic
[‡] Present address: 1. Physikalisches Institut, Universität Stuttgart, Pfaffenwaldring 57, 70550 Stuttgart, Germany
E-mail: slageren@pi1.physik.uni-stuttgart.de
Supporting information for this article is available on the WWW under http://www.eurjic.org or from the author.

π* level lies lower than d_{yz} and the lowest-energy transition is the "classical" metal-to-ligand charge transfer (MLCT or d→π*) transition (Scheme 1, C). The same situation is encountered if a weakly π-accepting chelate ligand is combined with co-ligands of medium to high donor strength such as in [(bpym)Pt(CN)$_2$] (bpym = 2,2′-bipyrimidine),[17] [(bpy)Pt(pz)$_2$] (pz = pyrazolates),[6] or [(terpy)Pt(X)]$^+$ (terpy = 2,2′:6′2′′-terpyridine, X = Cl, OH, SCN,[24−26] or alkynyl).[27]

If the co-ligands are no longer innocent, as assumed for the previous cases, but provide high-lying, filled p or π orbitals, the HOMO may have significant to dominating co-ligand contributions, admixed to platinum 5d orbitals, and the resulting lowest transition is assigned to a ligand-to-ligand charge transfer (L′LCT) (Scheme 1, D).[28] Since the HOMO has mixed metal/ligand character, it is also referred to as "mixed metal/ligand-to-ligand" charge transfer (MML′LCT).[7] Examples are the well-known dithiolate complexes such as [(bpy)Pt(mnt)] (mnt = malonitriledithiolate), where the HOMO is mainly formed by the p orbitals of the sulfur ligator atoms.[5,7,29−31] The same situation occurs when the co-ligands are unsaturated hydrocarbons such as phenyl or alkynyl. The π orbitals of the unsaturated system might act as the HOMO (Scheme 1, D). On the other hand back-bonding from Pt to the π* orbitals of the substituents should lower the electron density at the platinum atom with resulting destabilisation of the d orbitals. The situation then approaches case C. So far lowest absorption bands of such compounds containing aryl or alkynyl substituents have been assigned to "classical" MLCT transitions with no contribution from the π orbitals other than (small) π back-bonding.[1,3,27] The MLCT assignment is based on the fact that the absorption maxima increase with increasing energy of the diimine π*-orbital, E_{max} (complex): tmphen > dmphen > phen > bpy > dppz > tap. In the series of an individual diimine ligand the absorption energy increases slightly from methyl to mesityl and markedly from mesityl to phenyl. This parallels the electron donating ability of the substituents, upon which the platinum d orbitals are destabilised, decreasing the energies of the absorption maxima. However, we recently reported on a series of electron rich organoplatinum complexes with diazabutadiene ligands [(R′-DAB)PtR$_2$] (R′-DAB = *N*,*N*′-disubstituted 1,4-diazabutadienes, R′ = aryl or alkyl, R = alkyl, aryl or alkynyl) which were proven to exhibit low-lying L′LCT transitions.[19] It was shown, that the lowest transition gradually changes character from MLCT to L′LCT due to the contribution of the co-ligands to the HOMO. With increasing electron-donating ability of the alkyl co-ligands, the character of the lowest transition gradually obtains partial σ-bond-to-ligand (SBLCT or σ→π*) character with consequent photolability of such complexes. The corresponding aryl and alkynyl complexes have much larger contributions of the co-ligand to the highest filled orbitals and the lowest transitions therefore have mixed MLCT/L′LCT character.

An appropriate choice of diimine chelate ligand and co-ligands should therefore allow predetermination of the characters of the lowest energy transitions and lowest emitting states in such molecules.

This paper reports a combined experimental and theoretical study including absorption and emission spectroscopy together with quantum chemical calculations to determine the character of electronic transitions in a broad series of electron-rich platinum complexes of the type [(N^N)PtR$_2$] with R = alkyl, alkynyl, phenyl or mesityl (2,4,6-trimethylphenyl). The diimine ligands (N^N) range from the very good accepting aliphatic diimine ligands R′-DAB (*N*,*N*′-disubstituted diazabutadienes) to relatively electron-rich ones such as 1,10-phenanthroline (phen) and derivatives. The aim was to ascertain the extent to which the co-ligands contribute to the frontier orbitals and hence to the excited state, and, secondly, if emission spectroscopy can give a clue as to the excited state character.

Results and Discussion

The dimethylplatinum complexes were chosen as a means to render the platinum centre electron-rich without the possibility of π-electron contribution. Phenyl, mesityl and the alkynyl co-ligands C≡CR (R = *t*Bu or Ph) can potentially interact with the diimine ligands via their π systems. A special reason to use mesityl co-ligands comes from the fact that they provide steric shielding of the complexes axial positions and therefore prevent stacking or dimer formation, which simplifies assignment. Earlier, we reported that they emit light much more effectively than their diphenyl or dimethyl analogues,[21] which was recently used by Kane−Maguire and Wright to study energy- and electron-transfer processes in such systems.[2] The diimine ligands which were chosen are depicted in Scheme 2. Complexes of phenanthroline ligands are known to exhibit more long-lived emissions compared to their bpy analogues and the diazabutadienes (DAB), due to their rigidity which leads to decreased vibrational overlap between ground and excited states and concurrent slow nonradiative decay.[32] Introduction of the methyl substituent to phenanthroline increases the electron density in these ligands (4,7-dmphen and tmphen). Substitution on the 2,9-positions gives additionally rise to steric interactions (repulsions) with the bulky mesityl groups and yields the highly distorted complex [(2,9-dmphen)PtMes$_2$]. Its molecular structure, as determined from X-ray crystallography, shows marked deviation from the square-planar environment of the metal atom.[33] The use of the tap ligand [34−38] was motivated by the aim to decrease the electron density by the introduction of two further nitrogen atoms, but at the same time maintain the above described rigidity of a phenanthroline type of ligand. The dppz ligand is known to form emissive transition metal complexes which display different types of lowest excited states depending on the metal fragment (^{3}MLCT or $^3\pi-\pi^*$).[39] Furthermore such complexes can intercalate between DNA base pairs and might be used as DNA sensors.[40−42] The crystal structure of [(dppz)PtMes$_2$] was recently reported and shows π-stacking of pairs of two molecules in the unit cell.[43]

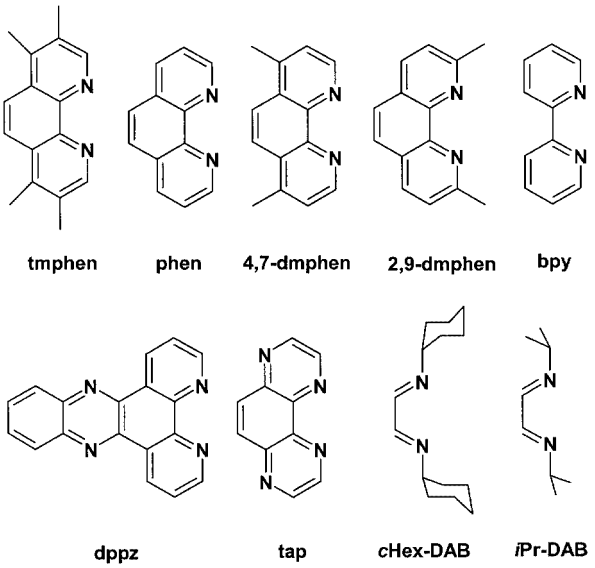

Scheme 2. Representation and nomenclature of the diimine ligands used: tmphen = 3,4,7,8-tetramethyl-1,10-phenanthroline, phen = 1,10-phenanthroline, 4,7-dmphen = 4,7-dimethyl-1,10-phenanthroline, 2,9-dmphen = 2,9-dimethyl-1,10-phenanthroline, bpy = 2,2′-bipyridine, dppz = dipyrido[3,2-*a*:2′,3′-*c*]phenazine, tap = 1,4,7,10-tetrazazaphenanthrene (pyrazino[2,3-*f*]quinoxaline), *c*Hex-DAB = *N*,*N*′-dicyclohexyl-1,4-diazabutadiene (*N*,*N*′-dicyclohexyl-1,2-ethanediimine), *i*Pr-DAB = *N*,*N*′-diisopropyl-1,4-diazabutadiene (*N*,*N*′-diisopropyl-1,2-ethanediimine)

Crystal Structure Determination of [(tmphen)PtMes$_2$], [(tap)PtPh$_2$], and [(bpy)PtMe$_2$]

The molecular structure and intermolecular phenomena such as Pt−Pt interaction or π−π stacking of the aromatic diimine ligands have a strong impact on the emission properties of molecules of the type which is presently under study.[10,12,44] Therefore, the results are discussed of a single-crystal X-ray diffraction study on [(tmphen)PtMes$_2$] (Figure 1), [(tap)PtPh$_2$] (Figure 2) and [(bpy)PtMe$_2$] (Figure 3),

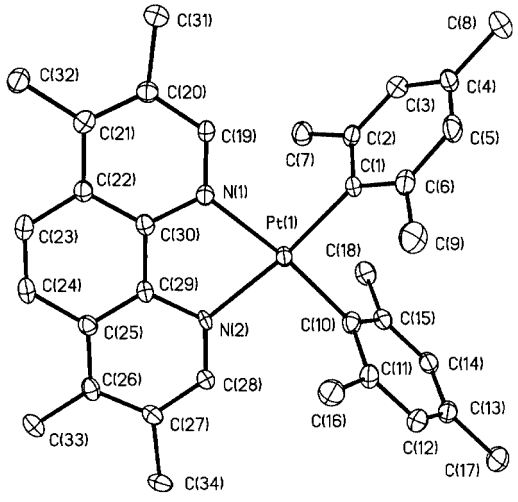

Figure 1. View of [(tmphen)PtMes$_2$] from crystal structure determination (with numbering); the atoms are represented by 50% thermal ellipsoids

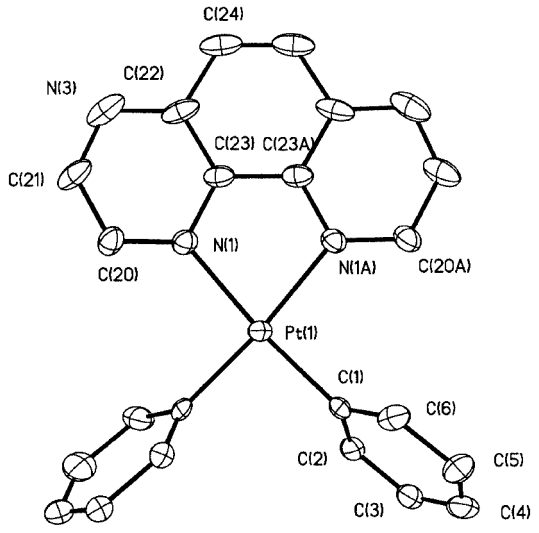

Figure 2. View of [(tap)PtPh$_2$] from crystal structure determination (with numbering); the atoms are represented by 50% thermal ellipsoids

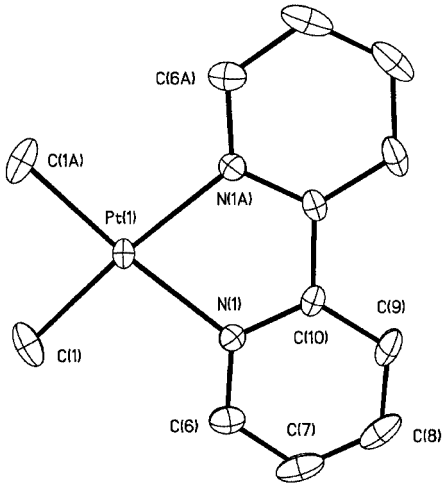

Figure 3. View of [(bpy)PtMe$_2$] from crystal structure determination (with numbering); the atoms are represented by 50% thermal ellipsoids

of which the first two are previously unpublished structures. The structures were solved and refined with the results shown in the Supporting Information (see also the footnote on the first page of this article). Table 1 lists some selected structural parameters of these complexes.

The molecular structures of all three complexes are quite similar. That of the tmphen complex fits into the series of other dimesitylplatinum complexes so far characterized by X-ray diffraction such as [(bpy)PtMes$_2$],[45] or [(phen)PtMes$_2$],[46] and [(dppz)PtMes$_2$].[43] The crystal and molecular structure of [(bpy)PtMe$_2$] (Figure 6) has been reported before,[47] our results being essentially the same but more precise. The chelate "bite" angle in all these compounds lies between 78 and 79° and the Pt−N distances and other structural parameters within the chelate ligands do not vary significantly. The aryl substituents in the mesityl and phenyl complexes show a tilt angle towards the co-

Table 1. Selected structural parameters for [(tmphen)$PtMes_2$], [(tap)$PtPh_2$] and [(bpy)$PtMe_2$]

[(tmphen)$PtMes_2$]		[(tap)$PtPh_2$]		[(bpy)$PtMe_2$]	
	Distance [Å]		Distance [Å]		Distance [Å]
Pt1−C1	2.031(7)	Pt−C1	1.995(9)	Pt1−C1	2.040(6)
Pt1−C10	2.024(7)		−	−	
Pt1−N1	2.103(5)	Pt−N1	2.113(7)	Pt1−N1	2.094(4)
Pt1−N2	2.111(6)		−	−	
C29−C30	1.427(9)	C23−C23A	1.43(2)	C10−C10A	1.477(8)
C23−C24	1.340(11)	C24−C24A	1.33(3)		−
$C_{Mes}-C_{Mes}$[a]	1.394(10), 1.402(11)	$C_{Ph}-C_{Ph}$[a]	1.39(2)		−
Pt1−C_{ortho} [b]	3.268(10), 3.282(10)				
	Angle [°]		Angle [°]		Angle [°]
C10−Pt1−C1	90.7(3)	C1−Pt−C1A	91.0(6)	C1−Pt−C1A	87.8(5)
N1−Pt1−N2	78.6(2)	N1−Pt−N1A	79.4(4)	N1−Pt−N1A	78.2(2)
C10−Pt1−N1	173.6(2)	C1−Pt−N1	174.2(3)	C1−Pt−N1	175.1(2)
C1−Pt1−N1	95.1(2)	C1−Pt−N1A	94.8(4)	C1−Pt−N1A	97.0(3)
	Dihedral angle [°]		Dihedral angle [°]		Dihedral angle [°]
Mes/co-plane[c]	70.2, 68.7	Ph/co-plane	68.7		−
Mes/Mes	81.7	Ph/Ph	86.3		−
Py/Py[d]	2.0	Pz/Pz[d]	1.2	Py/Py[d]	2.0

[a] Averaged values for $C_{aryl}-C_{aryl}$ distances. [b] Closest contacts to *ortho*-C atoms of the two mesityl substituents. [c] The coordination plane as defined by C1, C10, N1, N2 and Pt1. [d] Defined by the six-membered rings which form (approximately) half the ligand.

ordination plane of about 68−70°. Similar tilt angles were also found for [(dpp)$PtPh_2$] [dpp = 2,3-bis(2-pyridyl)pyrazine].[13] This means, that the aryl tilt angle is not governed by the steric strain from the methyl substituent. Furthermore in view of the above-mentioned similar structures which exhibit different symmetry, space groups and packing of the molecules it is unlikely that the tilt angle has its origin in crystal packing effects, but is indeed the optimal molecular geometry. Recent calculations showed, that this tilt angle is crucial for the calculated energies and characters of the MOs and hence the electronic transitions in such complexes[19,33,48] The only difference between the mesityl and the phenyl complexes is the shorter Pt−N bond of the phenyl derivative. A similar observation was made for the complex [(2,9-dmphen)$PtPh_2$] in comparison to the mesityl analogue.[33]

Intermolecular interactions are of importance for optical spectroscopy. Therefore we examined the crystal structures of the complexes in that respect. In square-planar platinum(II) complexes, two intermolecular interactions are important, namely π interactions of the aromatic α-diimine ligands and Pt···Pt interactions. The tmphen complex forms dimers in the unit cell, which are π-stacked in a non-graphite-like fashion, with an interplanar distance of 3.52(1) Å (Figure 4). Perhaps due to their methyl substituents the ligands are not ordered back-to-back but offset. For the [(dppz)$PtMes_2$] complex a graphite-like stacking with the formation of dimers was observed with a interplanar distance of 3.427(2) Å,[43] not very different from that of the chloro derivative [(dppz)$PtCl_2$] of about 3.45 Å[49] and

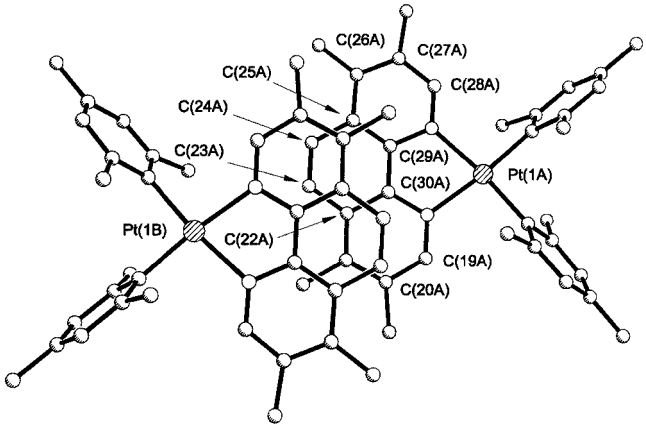

Figure 4. View of two molecules packing in [(tmphen)$PtMes_2$]

graphite (3.354 Å). In [(tap)$PtPh_2$] again a different π-stacking is observed (Figure 5). The ligand planes intersect much more and there is no diagonal offset like for the tmphen complex. Also in contrast to the tmphen complex the molecules form indefinite stacks along the crystallographic *c* axis, with the interplanar distance being only 3.056(2) Å. Although the structure of [(bpy)$PtMe_2$] was published,[47] the crystal packing was not discussed. In fact, the complex exhibits quite a complex stacking behaviour (Figure 6). The distance between the planes of the ligand is 3.45(1) Å. Interestingly, this behaviour does not resemble that of the dichloro complex [(bpy)$PtCl_2$] which occurs either in the red form with strong Pt···Pt interaction (*d* = 3.45 Å) but no π

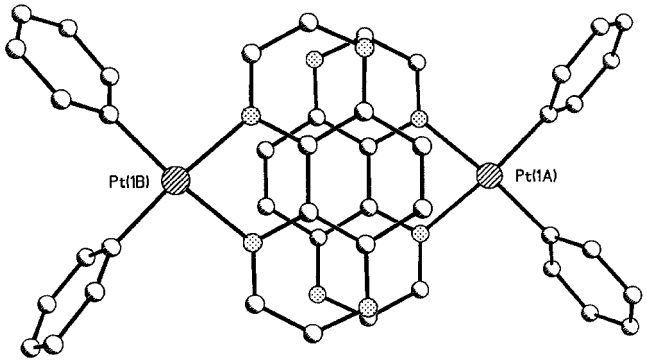

Figure 5. View of two molecules packing in [(tap)$PtPh_2$]

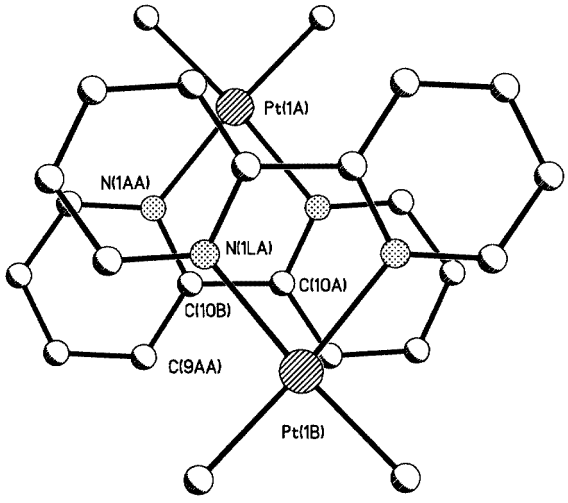

Figure 6. View of two molecules packing in [(bpy)$PtMe_2$]

interaction [50] or the yellow form with longer Pt···Pt distances of 4.5 Å and stacking of each one pyridyl unit.[51] These two polymorph types are also found in a series of (diimine)platinum complexes with Cl, CN, NCS, NCO as substituents.[44]

The Pt···Pt distances vary from complex to complex. In the tmphen complex, it is 9.331(3) Å within the dimer, and the shortest Pt···Pt distance with 6.465(3) Å is found between adjacent stacks. In case of the dppz complex the shortest Pt···Pt distance is 7.784(4) Å. The tap complex, in which the molecules are not diagonally offset like in the tmphen derivative, the Pt···Pt distance within the stacks is slightly shorter at 7.673(2) Å. The shortest Pt···Pt distance is between adjacent stacks [6.465(3) Å]. The Pt···Pt distance in the bpy complex is 5.496(3) Å, longer than the distances in either form of the dichloro complex.

From these data we can conclude that no strong Pt···Pt interactions are present in the molecules in their crystalline form, and the only possible intermolecular interaction is that of π stacking. This type of interaction can cause excimer formation. This will be further discussed in the emission spectroscopy section (see below). The DFT-calculated bond lengths and angles fit the experimentally obtained ones for [(bpy)$PtMes_2$],[45] and [(bpy)$PtMe_2$] well.

Absorption Spectroscopy and Calculations

The complexes [(α-diimine)PtR_2] (R = Me, Ph, or Mes) exhibit broad and partly structured long-wavelength absorption bands (Figure 7).[2,19−21,52] These bands show negative solvatochromism, indicating their charge transfer character (Table 2). The absorption bands of the complexes can be divided into two sets, one in the visible and one in the near UV, which are denoted by CT(1) and CT(2), respectively. For the corresponding R′-DAB (DAB = 1,4-diaza-butadiene) complexes it was shown that the various absorptions within one set are due to the presence of several electronic transition rather than vibronic structuring.[19] CT(1) always consists of several components which are all of moderate to weak intensity. The second band system [CT(2)] is always stronger than the first one and less structured. The energies of the absorption maxima increase with the diimine π*-level energy, and decrease with increasing electron-donating abilities of the co-ligands.

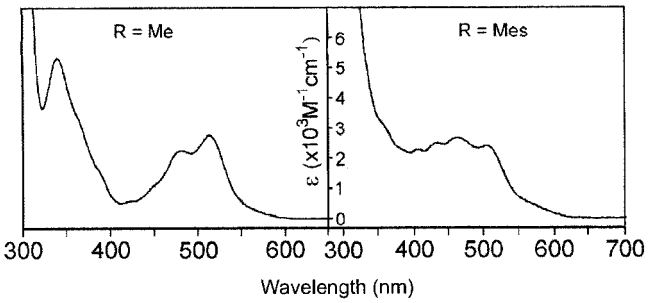

Figure 7. Absorption spectra of [(bpy)$PtMe_2$] (left) and [(bpy)$PtMes_2$] (right) in toluene solution

In order to assign the absorption bands, and in particular to determine the co-ligand contributions to the highest occupied MOs (HOMO), DFT calculations were performed on two complexes, namely [(bpy)$PtMe_2$] and [(bpy)$PtMes_2$]. As expected, the lowest unoccupied MOs (LUMO) are calculated to be almost exclusively located on bpy, even more so than in the case of the corresponding *i*Pr-DAB complexes (Tables 3 and 4).[19] This is due to the lower electron density on the coordinating nitrogen atoms in the case of bpy which limits delocalization of the frontier orbitals. The methyl contribution to the highest occupied MOs is quite limited (Table 3), making them almost purely metal-centred in character.

For the mesityl derivative the calculations yield a markedly changed situation. The HOMO 47a has mixed Pt-5d/mesityl-π orbital character and the following HOMOs are of almost pure π_{Mes} character and only one more or less pure d_{Pt} orbital has remained. Hence, like in the case of the *i*Pr-DAB complexes, also the highest occupied MOs of arylplatinum(II) complexes of aromatic α-diimines have predominant co-ligand character. This is at variance with the metal character which is generally assumed in literature.

The TD-DFT-calculated lowest transitions of [(bpy)$PtMe_2$] can be described as having mainly d_{Pt}-π*(bpy) (MLCT) character in agreement with the "classical" assign-

Table 2. Long-wavelength absorption maxima of platinum complexes

Compound[a]	CT(2)			CT(1)	
	λ_5 (ε)	λ_4 (ε)	λ_3 (ε)	λ_2 (ε)	λ_1 (ε)
[(*c*Hex-DAB)$PtMe_2$]	402 (3.4)	471sh (0.3)	498 (1.2)	535 (2.1)	577 (2.6)
[(*c*Hex-DAB)$PtMes_2$]	361 (3.6)	467 (3.4)	508 (3.5)	542 (3.6)	602sh (2.5)
[(bpy)$PtMe_2$]	340 (5.2)	423 (0.9)	454sh	482 (2.64)	513 (2.81)
[(bpy)$PtMes_2$]	352 (3.1)	406 (2.31)	432 (2.48)	459 (2.69)	504 (2.46)
[(bpy)$PtPh_2$]	341 (3.79)	388 (1.90)	416 (1.46)	454 (2.43)	480 (3.12)
[(tmphen)$PtMe_2$]	324 (4.98)	–	360sh (2.0)	450 (3.77)	477 (3.68)
[(tmphen)$PtMes_2$]	331 (4.12)	345 (3.38)	398 (3.71)	444 (3.38)	469 (3.06)
[(tmphen)$PtPh_2$]	336 (2.59)	346 (2.36)	384 (2.1)	428sh (2.8)	448 (2.98)
[(phen)$PtMe_2$]	330 (5.04)	364 (2.41)	450 (2.96)	470 (3.15)	509 (3.62)
[(phen)$PtMes_2$]	336sh (3.0)	–	420 (3.62)	447 (3.04)	500 (2.80)
[(phen)$PtPh_2$]	395 (2.26)	–	–	459sh (3.01)	477 (3.54)
[(dppz)$PtMe_2$]	362 (13.1)[b]	377 (12.3)[b]	450 (2.96)	480 (3.05)	521 (3.42)
[(dppz)$PtMes_2$]	362 (12.9)[b]	378 (12.3)[b]	436 (3.84)	471sh (3.12)	513 (2.75)
[(dppz)$PtPh_2$]	363 (12.1)[b]	379 (12.3)[b]	–	463 (2.79)	483 (2.83)
[(TAP)$PtMe_2$]	385 (2.34)	–	480 (2.43)	508sh (2.3)	554 (2.45)
[(TAP)$PtMes_2$]	375sh (3.4)	408 (3.02)	470 (3.31)	498 (3.42)	567 (2.83)
[(TAP)$PtPh_2$]	–	432 (2.38)	454sh (2.2)	503sh (2.1)	533 (2.51)
[(2,9-dmphen)$PtMes_2$]	274 (28)[b]	293 (16.7)[b]		418 (2.45)	497 (2.13)
[(2,9-dmphen)$PtPh_2$]	273 (29)[b]		384 (3.08)	438 (2.56)	461 (2.59)
[(4,7-dmphen)$PtMes_2$]	268 (26)[b]	338 sh	406 (2.96)	448 (2.69)	481 (2.50)

[a] Absorption maxima in wavelength [nm] from measurements in toluene solution. The molar extinction coefficients ε are given in parentheses [1000 $M^{-1}cm^{-1}$]. [b] Intraligand transitions.

Table 3. ADF/BP calculated one-electron energies and percentage composition of selected highest occupied and lowest unoccupied molecular orbitals of [(bpy)$PtMe_2$] expressed in terms of composing fragments

MO	*E* [eV]	Prevailing character	Pt	Me	bpy
Unoccupied					
$7a_2$	−2.18	π* bpy	3 (d_{xy})	–	97
$10b_1$	−2.45	π* bpy	3 (d_{xz})	–	96 (π*)
$9b_1$	−3.14	π* bpy	9 (d_{xz})	–	90 (π*)
Occupied					
$21a_1$	−4.53	d_{Pt}	24 (s), 54 ($d_{x^2-y^2}$), 14 (d_{z^2})	8	–
$6a_2$	−4.60	d_{Pt}	85 (d_{xy})	8	6
$8b_1$	−4.98	d_{Pt}	76 (d_{xz})	6	17
$20a_1$	−5.02	d_{Pt}	15 ($d_{x^2-y^2}$), 63 (d_{z^2})	18	3
$17b_2$	−6.04	sp^3 (Me)	18 (d_{yz}), 1 (p_y)	46	31
19a1	−6.15	sp^3 (Me)	5 (s), 3 (p_z), 15 ($d_{x^2-y^2}$)	59	18
$5a_2$	−6.66	π bpy	–	–	99

ment. The calculated energies agree only moderately with the experimentally found ones (Table 5). One reason is the strong solvatochromism of the compounds, as displayed by the shift of the experimental energies going from toluene to pentane as solvent. However, they agree at least qualitatively, showing a number of low energy transitions of weak to moderate intensity which can be found in the range of 420−520 nm in the spectra, and a stronger transition which

Table 4. ADF/BP-calculated one-electron energies and percentage composition of selected highest occupied and lowest unoccupied molecular orbitals of [(bpy)$PtMes_2$] expressed in terms of composing fragments

MO	*E* [eV]	Prevailing character	Pt	Mes	bpy
Unoccupied					
48b	−0.65	Mes + Pt	6 (p_y), 16 (d_{yz})	64	13
49a	−1.33	π* bpy	–	1	98
48a	−2.50	π* bpy	2 (d_{xy})	–	98
47b	−2.75	π* bpy	2 (d_{xz})	–	97 (π*)
46b	−3.51	π* bpy	6 (d_{xz})	–	93 (π*)
Occupied					
47a	−4.62	Mes + Pt	3 (s), 2 (d_{xy}), 19 ($d_{x^2-y^2}$), 9 (d_{z^2})	67	–
46a	−5.03	d_{Pt}	19 (s), 37 ($d_{x^2-y^2}$), 28 (d_{z^2})	15	–
45b	−5.14	π (Mes)	10 (d_{xz})	88	2
44b	−5.26	π (Mes)	2 (d_{xz})	98	–
45a	−5.35	Mes	6 (d_{xy})	93	–
44a	−5.45	d_{Pt}	79 (d_{xy}), 3 (d_{z^2})	11	6
43b	−5.74	d_{Pt}	70 (d_{xz})	19	11
43a	−6.53	Mes	2 (s), 2 (p_z), 3 ($d_{x^2-y^2}$), 8 (d_{z^2})	68	16
42a	−6.81	d_{Pt} + Mes	1 (s); (p_z), 21 ($d_{x^2-y^2}$), 26 (d_{z^2})	52	–
37a	−6.98	π bpy	–	–	99

Table 5. Selected calculated lowest TD-DFT singlet excitation energies [eV] for [(bpy)$PtMe_2$] compared to experimental absorption data

State	Main character [%]	ADF/BP		Experiment		
		Transiton energy [eV]	Osc. strength	Transiton energy [eV][a]	Transition energy [eV][b]	Extinction coeff. [M^{-1} cm^{-1}][b]
$^1A_1$	75 ($8b_1 \rightarrow 9b_1$), 16 ($6a_2 \rightarrow 7a_2$),	2.17	0.017	2.22	2.42	2810
$^1B_2$	97 ($6a_2 \rightarrow 10b_1$)	2.42	0.010	2.42	2.57	2640
$^1B_2$	95 ($8b_1 \rightarrow 7a_2$)	2.96	0.036	3.10	3.26	2410(sh)
$^1A_1$	40 ($8b_1 \rightarrow 10b_1$), 30 ($6a_2 \rightarrow 7a_2$), 20 ($8b_1 \rightarrow 9b_1$)	3.15	0.152	3.53	3.65	5200
$^1A_1$	92 ($6a_2 \rightarrow 8a_2$);	3.65	0.041	4.43	4.13	5800(sh)

[a] Measured in pentane. [b] In toluene.

Table 6. Selected calculated lowest TD-DFT singlet excitation energies [eV] for [(bpy)$PtMes_2$] compared to experimental absorption data

State	Main character [%]	ADF/BP		Experiment[a]	
		Transition energy [eV]	Osc. strength	Transition energy [eV]	Extinction coeff. [M^{-1} cm^{-1}]
^1A	48 ($44b \rightarrow 47b$), 36 ($43b \rightarrow 46b$)	2.50	0.011	2.46	2460
^1A	44 ($44b \rightarrow 47b$), 30 ($43b \rightarrow 46b$)	2.56	0.031	2.70	2690
^1B	67 ($44a \rightarrow 47b$), 28 ($44b \rightarrow 48a$)	2.75	0.006	2.87	2480
^1A	46 ($43b \rightarrow 47b$), 32 ($44a \rightarrow 48a$), 10 ($43b \rightarrow 46b$)	3.39	0.172	3.52	3100

[a] Measured in toluene.

can be recognized in the dominant band at about 340 nm in the spectra.

As a consequence of the mixed-metal/co-ligand character of the highest occupied MOs of [(bpy)$PtMes_2$], its electronic transitions have mixed L′LCT/MLCT character, where both contribute in roughly equal measures (Table 6). Interestingly, these are directed towards different π* orbitals of bpy. Again, the transition energies and oscillator strengths show only qualitative agreement with the observed values as above.

Emission Spectroscopy

Most of the assignments of excited states and electronic transitions in (diimine)platinum complexes are based on emission studies,[1,3,6−8,12,18,27] since the collected data, such as emission lifetimes, quantum yields, apparent Stokes shifts etc., allow easy discrimination between ligand-field (LF), intra-ligand (π-π*) and charge-transfer excited states. Here we use emission spectra both at room temperature and in low-temperature solvent glasses to probe for any differences in excited-state properties between the methyl complexes on one side and the aryl derivatives on the other. The room-temperature emission data of the complexes are reported in Table 7. None of the DAB or tap complexes proved to be emissive in fluid solution at room temperature. Furthermore, only two of the methyl complexes (tmphen and dppz) showed luminescence under these conditions. For all other complexes emission was observed as broad unstructured bands, albeit with low quantum yields between 10^{-5} and 10^{-3}. The excitation spectra (Figure 8) show that the observed emission bands are indeed due to the complexes. Comparing the three different types (Me, Mes, and Ph) of complexes it can be seen that the methyl complexes are the poorest emitters, followed by the phenyl complexes, which have quantum yields that are a by factor of 3−5 higher. The mesityl complexes show the highest luminescence efficiency with quantum yields of a factor of 5−10 higher than those of the corresponding methyl complexes. Considering the low quantum yield, the excited-state decay is mainly governed by nonradiative processes, which are apparently more efficient for the methyl complexes than for the aryl ones. Transient absorption and time-resolved emission measurements under these conditions showed that the lifetimes were shorter than our instrument resolution (5 ns). Another interesting observation is that while for both the methyl and mesityl complexes the apparent Stokes shifts are mostly above 6000 cm^{-1}, those of the phenyl complexes are much lower at around 3000 cm^{-1}. Apparently, the phenyl complexes are much less distorted in their excited states than the other ones. Decrease in excited state distortion should lead to slower nonradiative decay by decrease of vibrational overlap. However no increase in quantum yield, which would be the consequence, was observed for the phenyl derivatives.

Apart from these general observations, some interesting peculiarities can be observed. The sterically overcrowded complex [(2,9-dmphen)$PtMes_2$] emits only very weakly at rather high energy with a resulting Stokes shift of 3000

Table 7. Luminescence quantum yields at 298 K

Compound[a]	$\lambda_{abs,max}$	λ_{em}	Stokes shift [cm^{-1}]	Φ[b]
[(tmphen)$PtMe_2$]	464	714	7550	0.00071
[(dppz)$PtMe_2$]	505	760	6650	0.00060
[(tmphen)$PtMes_2$]	457sh, 436	620	5750	0.00984
[(dppz)$PtMes_2$]	492sh, 424	765	7250	0.00210
[(4,7-dmphen)$PtMes_2$]	466sh, 438	657	6240	0.00542
[(phen)$PtMes_2$]	482	688	6220	0.00258
[(bpy)$PtMes_2$]	481	687	6230	0.00227
[(2,9-dmphen)$PtMes_2$]	472	550	3005	0.00073
[(dppz)$PtPh_2$][c]	483	605	4175	0.02710
[(dppz)$PtPh_2$]	464	517	2210	0.00255
[(dppz)$PtPh_2$]	464	760	8350	0.00171
[(dppz)$PtPh_2$][d]	464	550	3370	—[e]
[(tmphen)$PtPh_2$]	442	518	3320	0.00239
[(phen)$PtPh_2$]	456	524	2850	0.00123
[(bpy)$PtPh_2$]	453	522	2920	0.00107
[(2,9-dmphen)$PtPh_2$]	445	516	3090	0.00024

[a] From measurements in THF solution. $\lambda_{(abs,max)}$ = long-wavelength absorption maximum [nm]. $\lambda_{(ex)}$ = excitation wavelength. [b] Φ = emission quantum yield relative to $[(bpy)_3Ru]^{2+}$ in MeCN solution ($\Phi = 0.062$).[61] [c] In toluene solution. [d] Dilute. [e] Not determined.

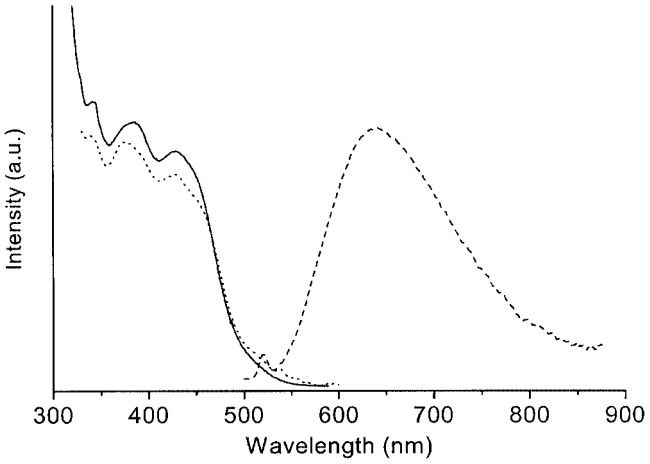

Figure 8. Absorption (——), emission (----) and excitation spectrum (····) of [(tmphen)$PtMes_2$] in CH_2Cl_2 solution

cm^{-1}. Methyl substitution of phenanthroline ligand increases the emission energies and the quantum yields of the mesityl complexes as demonstrated by the series phen < 4,7-dmphen < tmphen, which can be attributed to the energy gap law. The compound [(dppz)$PtPh_2$] exhibits a complex behaviour. In THF solution, at a concentration of 10^{-5} mol/L, two emission maxima were observed at 517 and 760 nm, respectively. After dilution to approx. 10^{-6} mol/L, the 760-nm band disappeared and a weak band was observed at 550 nm with the 517-nm band more or less unchanged. The band at 550 nm seems to be similar to those of the other complexes and we therefore assign the very-long-wavelength emission at 760 nm to excimer emission. The high-energy component at 517 nm might originate from a ligand-centered ($^3\pi$-π^*) state. In toluene solution also an emission at rather low energy is observed with a relatively high quantum yield. No change in emission maximum was observed on dilution. Most probably the excited molecule interacts with toluene molecules. This is in accordance with the observation that dppz complexes readily form dimeric π stacks,[43] and also strongly interact with aromatic solvent molecules such as toluene.[43] Possibly the deviating behaviour of this complex can be traced to its different excited state character (see below).

At low temperature (90 K) in glassy frozen 2-MeTHF, all the examined mesityl- and methylplatinum complexes, upon irradiation into their lowest absorption bands, show broad emissions with lifetimes of mostly some μs (Table 8). They were only very slightly structured. As an example the time-resolved spectra of [(tmphen)$PtPh_2$] are depicted in Figure 9. The Stokes shifts were all in the same range (4000−6000 cm^{-1}). The DAB complexes have the shortest emission lifetimes. This and the highest Stokes shift in the series reflect the high flexibility of the R′-DAB ligand, which allows rapid non-radiative decay. Similar differences have been recently observed for tetramethylplatinum(IV) complexes, where the tmphen derivative exhibited an enormously increased lifetime (9.3 μs) compared to the *c*Hex-DAB analogue (44 ns).[32] The lowest-energy emissions of all other complexes have lifetimes which are all in the same range. Solid-state data for the mesityl complexes of bpy (τ = 0.9 μs), phen (1.8 μs) and tmphen (2.1 μs) have been reported in literature, which compare well with the present numbers.[2] Interestingly, no differences are observed between the methyl complexes on one hand, and the aryl ones on the other. This means that the difference in excited-state character is not reflected in emission lifetimes. For [(dppz)$PtPh_2$] the lowest excited state is clearly of intra-ligand (phenazine) character. This might account for the peculiar behaviour at ambient temperature. In some cases on higher energy excitation longer-lived emission bands are observed at higher energies. These are often quite structured and we assign them to intraligand (IL) emissions. The fact that in some cases the lifetime is not much longer than that of the lowest-energy emission can be explained by the observation that even if the lowest excited state has IL character, its lifetime is of the same order of magnitude. For example, the emission of the yellow form of [(bpy)$PtCl_2$] in the solid state which is assigned to an $^3\pi$-π^* excited state has also a comparably low lifetime of only 3.5 μs compared to the phenanthroline analogue with 13.3 μs (both measured at 10 K).[8] Emission from higher excited states has been observed for other complexes at low temperatures, e.g. in (diimine)tungsten complexes.[53] Apparently, in all these cases radiative decay from a higher excited state is in competition with internal conversion or intersystem crossing to the lowest excited state.

The fact that the low-temperature lifetimes are not affected by the nature of the co-ligand, suggests that the differences in room-temperature emission quantum yield are due

Table 8. Low-temperature luminescence data

Compound[a]	Absorption: λ_{abs} [nm]	Excitation: λ_{exc} [nm]	Emission: λ_{em} [nm]	Stokes shift [cm^{-1}]	τ
[(N^N)PtMe$_2$]					
(*c*Hex-DAB)	370, 382, 474sh, 506, *542*	532	761	5310	8.3 ns
(*c*Hex-DAB)	370, 382, 474sh, 506, *542*	355	492, 525, *577*, 624sh	1120	1.7 μs
(bpy)	345sh, 427sh, 452, *484*	532	631	4810	3.1 μs
(bpy)	345sh, 427sh, 452, *484*	440	*523*, 559, 600sh	1540	8.0 μs
(tmphen)	352sh, 430, *460*	460	620	5610	2.5 μs
(dppz)	341, 359, 377, 462, *496*	450	640	4540	2.7 μs
[(N^N)PtMes$_2$]					
(*p*Tol-DAB)	485, 544, *588*	532, 355	815	4740	11 ns
(*c*Hex-DAB)	391, 407, 476 *506*	532	658sh, *734*	6140	68 ns
(*c*Hex-DAB)	391, 407, 476, *506*	532, 355	*584*, 607	2640	1.3 μs
(*i*Pr-DAB)	391, 407, 476, *506*	532	*737*, 796 sh	6190	51 ns
(tap)	429, 459, *522*, 591sh	532	684	4540	270 ns
(dppz)	414, 441, *475*, 532	440	*540*, 584, 635	2530	699 μs
(dppz)	414, 441, *475*, 532	532	582sh, *618*	4870	1.3 μs
(bpy)	366, 388, 411, 440, *472*	532	*584*, 607	4060	1.3 μs
(phen)	367, 388, 412, 441, *470*	532	*583*, 606	4120	1.4 μs
(tmphen)	391, 374, 388, 424, *449*	532, 440	*548*, 565	4023	2.7 μs
[(N^N)PtPh$_2$]					
(tmphen)	334sh, 408, *432*	440	501, *533*, 564sh	4390	7.9 μs
(dppz)	359, 374sh, 431, *456*	455	*540*, 584, 635	3410	782 μs

[a] From measurements at 90 K in glassy frozen 2-MeTHF solutions. The most intense component of the absorption or emission spectra is in italics and serves to calculate the Stokes shift. τ is the excited state lifetime as calculated from time-resolved measurements.

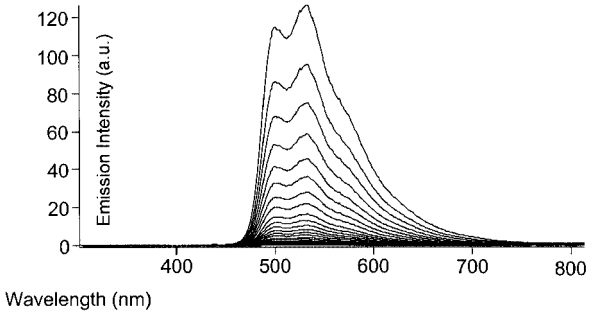

Figure 9. Time-resolved emission spectra of [(tmphen)PtPh$_2$] in MTHF glass at 110 K; λ_{exc} = 440 nm, *P* = 6.9 mJ, time delay between the spectra: 2000 ns

to thermally activated processes rather than traceable to the difference in excited-state character. It has been suggested that the rotation around the *o*-Me group in (α-diimine)mesitylplatinum(II) complexes could be such a thermally excited decay pathway. In the methyl and phenyl complexes clearly additional pathways must be present.

No differences between the methyl and aryl complex lifetimes at low temperature were found to indicate a difference in excited-state character. For example, the MLCT state of [(bpy)PtMe$_2$] has a lifetime of 3.1 μs at low temperatures, while that of the corresponding mesityl complex is slightly shorter at 1.3 μs. However, closer inspection of literature data reveals that in square-planar (α-diimine)platinum(II) complexes, the excited-state lifetime depends only weakly on the excited-state character. The excited states of [(3,3′-(CH$_3$OCO)$_2$bpy)PtCl$_2$] (τ = 1.1 μs),[8] and [(dmbpy)Pt(pz)$_2$] (dmbpy = 4,4′-dimethyl-2,2′-bipyridine; pz = dimethyl- or tetramethylpyrazole; τ = 1.8 or 0.4 μs, respectively)[6] were assumed to have MLCT character. However, the observed twist angle of 64(3)° of the pyrazolate groups relative to the binding plane in the above-mentioned complexes,[54] suggests that the π system of these pyrazolates may contribute significantly to the highest MOs. Alkynylplatinum(II) complexes have similar lifetimes, e.g. [(tmbpy)Pt(C≡C*p*Tol)$_2$] (τ = 1.3 μs, tmbpy = 4,4′,5,5′-tetramethyl-2,2′-bipyridine).[1] There is a number of indications that the alkynyl moiety is significantly involved in the excited state. Thus, DFT calculations on [(*i*Pr-DAB)Pt(C≡CH)$_2$] show over 60% participation of the alkynyl groups in the highest MOs. In addition, the excited state IR spectra of [(R′-bpy)Pt(C≡CR)$_2$] (R = Aryl, R′-bpy = alkyl-substituted bpy) shows a clear upward shift of the ν(C≡C) frequency of about 25−35 cm^{-1} compared to the ground states.[1] And finally, it was remarked that the photophysical behaviour of [(4,4′-*t*Bubpy)Pt(C≡CNMe)$_2$] "does not fit with the model of a lowest ^{3}MLCT excited state".[1] Other complexes which have excited states that are clearly different from purely MLCT, such as the (α-diimine)platinum(II) dithiolate complexes, which have ^{3}MML′LCT (^{3}L′LCT) lowest-excited

states, also have comparable emission lifetimes.[5] Finally, the IL emission of the above-mentioned yellow form of [(bpy)$PtCl_2$] has again a similar emission lifetime, namely 3.5 μs.

The only difference between the MLCT emissions of the methyl complexes and the L′LCT/MLCT emissions of the aryl complexes is the partial structuring of the emission bands of the latter complexes. This is rather unusual for ^{3}MLCT emissions of (diimine)platinum complexes.[3,5,8,18] Such structuring was also observed for the before-mentioned complexes [(dmbpy)$Pt(pz)_2$],[6] or [(tmbpy)Pt-(C≡CTol)$_2$],[1] which most probably have similar mixed L′LCT/MLCT excited states.

Conclusions

The DFT calculations showed that the lowest excited states of the methyl-substituted (α-diimine)platinum(II) complexes have virtually pure MLCT character. In contrast those of the corresponding phenyl and mesityl complexes were revealed to have mixed L′LCT/MLCT character. This is supported by the molecular structures from single-crystal XRD which show an optimum tilt angle for the aryl groups for effective ligand(aryl)-to-ligand(diimine) interaction. From the emission data, there were two differences in excited-state behaviour between these two types of complexes. Firstly, the room-temperature quantum yields are up to 10 times larger for the mesityl complexes, compared to the methyl derivatives. Secondly, a slight structuring of the emission bands was visible for the aryl derivatives, which could not be found for the methyl derivatives. The low-temperature emission lifetimes, however, do not depend on the nature of the co-ligand. It must therefore be concluded that emission spectroscopy is not a very sensitive tool to determine the excited-state character in (α-diimine)platinum(II) complexes. Techniques such as time-resolved IR spectroscopy are more promising in that respect. Furthermore, we have found from the combination of single-crystal XRD and concentration-dependent emission behaviour that for these electron-rich (diimine)platinum(II) complexes with alkyl, aryl or alkynyl ligand intermolecular Pt···Pt interactions do not occur and intermolecular π-stacking does only play a very minor role in sharp contrast to corresponding complexes with halide or pseudohalide ligands.

Experimental Section

Preparations: All preparations and manipulations were carried out under argon or nitrogen. The synthesis of the complexes [(*i*Pr-DAB)PtR_2] (R = alkyl, alkynyl or aryl) was recently described.[19] Other dimethyl and dimesityl complexes were prepared from [$(Me_2Pt(\mu\text{-}SMe_2)_2PtMe_2]$,[55] or [$(dmso)_2PtMes_2$],[56] respectively, as recently described for the DAB complexes.[20] The diphenylplatinum complexes were prepared from [(COD)$PtPh_2$],[57] as reported for various diimine ligands.[58] The compounds were thoroughly recrystallised to ensure the absence of impurities. They gave correct elemental analyses and ^{1}H NMR spectroscopy proved their identity and purity (see Supporting Information).

General Procedures for Crystal Structure Analyses: Suitable crystals of the complexes were obtained by slow concentration of saturated toluene solutions. For all three compounds, the data collection was performed at T = 183(2) K with a Siemens P4 diffractometer using Mo-K_α radiation (λ = 0.71073 Å). The absorption correction was done by ψ-scans. The structures were solved using the SHELXTL-PLUS package,[59] and refinement was carried out with SHELXL-97 employing full-matrix least-squares methods on F^2.[60] All non-hydrogen atoms were treated anisotropically, and hydrogen atoms were included by using appropriate riding models. Additional details on crystal data and structure refinement of [(tmphen)$PtMes_2$], [(tap)$PtPh_2$] and [(bpy)$PtMe_2$] can be found in the Supporting Information. CCDC-204746 [(bpy)$PtMe_2$], -204747 [(tap)$PtPh_2$], and -204748 [(tmphen)$PtMes_2$] contain the supplementary crystallographic data for this paper. These data can be obtained free of charge at www.ccdc.cam.ac.uk/conts/retrieving.html [or from the Cambridge Crystallographic Data Centre, 12, Union Road, Cambridge CB2 1EZ, UK; Fax: (internat.) + 44-1223/336-033; E-mail: deposit@ccdc.cam.ac.uk].

Instrumentation: ^{1}H NMR spectra for analytical purposes were recorded with a Bruker AC 250 spectrometer. UV/Vis absorption spectra were recorded with Bruins Instruments Omega 10, Hewlett−Packard 8453 Diode Array, or Varian Cary 4E spectrometers. Steady-state emission spectra were recorded with Spex Fluorolog or Spex Fluorolog 3 emission spectrophotometers, equipped with Peltier-cooled Hamamatsu 928 and 636−10 photomultiplier detectors, respectively. The solutions were deaerated by Ar purging for at least 20 min prior to measurement. The quantum yields were determined by comparison to [$(bpy)_3Ru]^{2+}$ in acetonitrile solution (Φ = 0.062),[61] and were found to be generally lower by the factor of 100 or more compared to this standard. Time-resolved emission spectra of samples in 2-MeTHF glasses (90 K) were recorded in an Oxford Instruments cryostat, using Spectra Physics GCR3 Nd:YAG or Coherent Infinity XPO lasers as excitation sources and an OMA detection system described elsewhere.[62] The solutions were prepared under nitrogen and freeze-pump-thaw-degassed three times before measurements.

Theoretical Calculations: The ground-state electronic-structure calculations on complexes [(bpy)PtR_2] (R = Me, Mes) were performed on the base of density functional theory (DFT) methods by using the ADF2000.2,[63,64] and Gaussian 98[65] program packages. The lowest excited states of the closed-shell complexes were calculated by the time-dependent DFT (TD-DFT) method (both ADF and G98 programs). Within the ADF program, Slater-type orbital (STO) basis sets of triple-ζ quality with polarization functions were employed, except for the methyl groups on the Mes ligands, which were described by basis sets of double-ζ quality with polarization functions. The inner shells were represented by frozen-core approximation (1s for C, N and 1s−4d for Pt were kept frozen). The following density functionals were used within ADF: the local density approximation (LDA) with VWN parametrisation of electron gas data or the functional including Becke's gradient correction[66] to the local exchange expression in conjunction with Perdew's gradient correction[67] to the LDA expression (ADF/BP). The scalar relativistic (SR) zero order regular approximation (ZORA) was used within this study.[68] Within Gaussian-98 Dunning's polarized valence double-ζ basis sets [69] were used for C, N and H atoms and quasirelativistic effective core pseudopotentials and corresponding optimized set of basis functions[70] for Pt. The hybrid Becke's three-parameter functional with the Lee, Yang and Parr correlation func-

tional (B3LYP) [71] was used in Gaussian 98 calculations (G98/B3LYP). Gaussian 98 was used for the calculations of the vibrations at G98/B3LYP optimised geometries. The calculations on [(bpy)$PtMe_2$] and [(bpy)$PtMes_2$] were performed in C_{2v} or C_2 constrained symmetries, respectively. The z axis was taken coincident with C_2 symmetry axis, while the platinum atom and bpy ligand lie in the yz plane. All results discussed correspond to optimised geometries.

Acknowledgments

This work was carried out in the framework of the COST D14 action. A. K. would like to thank Prof. D. J. Stufkens (University of Amsterdam) for the opportunity to do research in his group and also for fruitful discussions and Prof. W. Kaim is acknowledged for financial support. We are also grateful for a loan of K_2PtCl_4 by Johnson Matthey (JM). S. Z. thanks the Ministry of Education of the Czech Republic (OC.D14.20) for the financial support.

[1] C. E. Whittle, J. A. Weinstein, M. W. George, K. S. Schanze, *Inorg. Chem.* **2001**, *40*, 4053−4062.
[2] K. E. Dungey, B. D. Thompson, N. A. P. Kane-Maguire, L. L. Wright, *Inorg. Chem.* **2000**, *39*, 5192−5196.
[3] M. Hissler, W. B. Connick, D. K. Geiger, J. E. McGarrah, D. Lipa, R. J. Lachicotte, R. Eisenberg, *Inorg. Chem.* **2000**, *39*, 447−457.
[4] M. Hissler, J. E. McGarrah, W. B. Connick, D. K. Geiger, S. D. Cummings, R. Eisenberg, *Coord. Chem. Rev.* **2000**, *208*, 115−137.
[5] W. B. Connick, D. Geiger, R. Eisenberg, *Inorg. Chem.* **1999**, *38*, 3264−3265.
[6] W. B. Connick, V. M. Miskowski, V. H. Houlding, H. B. Gray, *Inorg. Chem.* **2000**, *39*, 2585−2592.
[7] W. Paw, S. D. Cummings, M. A. Mansour, W. B. Connick, D. K. Geiger, R. Eisenberg, *Coord. Chem. Rev.* **1998**, *171*, 125−150.
[8] V. M. Miskowski, V. H. Houlding, C.-M. Che, Y. Wang, *Inorg. Chem.* **1993**, *32*, 2518−2524.
[9] V. H. Houlding, V. M. Miskowski, *Coord. Chem. Rev.* **1991**, *111*, 145−152.
[10] V. M. Miskowski, V. H. Houlding, *Inorg. Chem.* **1991**, *30*, 4446−4452.
[11] V. M. Miskowski, V. H. Houlding, *Inorg. Chem.* **1989**, *28*, 1529−1533.
[12] W. Lu, M. C. W. Chan, K.-K. Cheung, C.-M. Che, *Organometallics* **2001**, *20*, 2477−2486.
[13] Y.-Y. Ng, C.-M. Che, S.-M. Peng, *New J. Chem.* **1996**, *20*, 781−789.
[14] C.-W. Chan, L.-K. Cheng, C.-M. Che, *Coord. Chem. Rev.* **1994**, *132*, 87−97.
[15] N. Chaudhury, R. J. Puddephatt, *J. Organomet. Chem.* **1975**, *84*, 105−115.
[16] A. Von Zelewsky, P. Belser, P. Hayoz, R. Dux, X. Hua, A. Suckling, H. Stoeckli-Evans, *Coord. Chem. Rev.* **1994**, *132*, 75−85.
[17] J. Biedermann, G. Gliemann, U. Klement, K.-J. Range, M. Zabel, *Inorg. Chem.* **1990**, *29*, 1884−1888.
[18] M. Maestri, D. Sandrini, V. Balzani, L. Chassot, P. Jolliet, A. Von Zelewsky, *Chem. Phys. Lett.* **1985**, *122*, 375−379.
[19] A. Klein, J. van Slageren, S. Záliš, *Inorg. Chem.* **2002**, *41*, 5216−5225.
[20] W. Kaim, A. Klein, S. Hasenzahl, H. Stoll, S. Záliš, J. Fiedler, *Organometallics* **1998**, *17*, 237−247.
[21] W. Kaim, A. Klein, *Organometallics* **1995**, *14*, 1176−1186.
[22] V. Balzani, A. Credi, M. Venturi, *Coord. Chem. Rev.* **1998**, *171*, 3−16.
[23] J. E. McGarrah, Y.-J. Kim, M. Hissler, R. Eisenberg, *Inorg. Chem.* **2001**, *40*, 4510−4511.
[24] J. A. Bailey, M. G. Hill, R. E. Marsh, V. M. Miskowski, W. P. Schaefer, H. B. Gray, *Inorg. Chem.* **1995**, *34*, 4591−4599.
[25] D. R. McMillin, J. J. Moore, *Coord. Chem. Rev.* **2002**, *229*, 113−121.
[26] J. F. Michalec, S. A. Bejune, D. G. Cuttell, G. C. Summerton, J. A. Gertenbach, J. S. Field, R. J. Haines, D. R. McMillin, *Inorg. Chem.* **2001**, *40*, 2193−2200.
[27] Q.-Z. Yang, L.-Z. Wu, Z.-X. Wu, L.-P. Zhang, C.-H. Tung, *Inorg. Chem.* **2002**, *41*, 5653−5655.
[28] A. Vogler, H. Kunkely, *Comments Inorg. Chem.* **1990**, *9*, 201−220.
[29] J. A. Weinstein, N. N. Zheligovskaya, M. Y. Mel′nikov, F. Hartl, *J. Chem. Soc., J. Chem. Soc., Dalton Trans.* **1998**, *15*, 2459−2466.
[30] Z. Hao, Z. Tang, Q. Shi, *Inorg. Chim. Acta* **1999**, *284*, 112−115.
[31] M. T. Cocker, R. E. Bachman, *Inorg. Chem.* **2001**, *40*, 1550−1556.
[32] J. van Slageren, D. J. Stufkens, S. Záliš, A. Klein, *J. Chem. Soc., Dalton Trans.* **2002**, 218−225.
[33] A. Klein, E. J. L. McInnes, W. Kaim, *J. Chem. Soc., Dalton Trans.* **2002**, 2371−2378.
[34] K. Karlsson, C. Moucheron, A. Kirsch-De Mesmaeker, *New J. Chem.* **1994**, *18*, 721−729.
[35] A. Kirsch-De Mesmaeker, R. M. D. Nasielski-Hinkens, D. Pauwels, J. Nasielski, *Inorg. Chem.* **1984**, *23*, 377−379.
[36] L. Jacquet, J. M. Kelly, A. Kirsch-De Mesmaeker, *J. Chem. Soc., Chem. Commun.* **1995**, 913−914.
[37] S. Ernst, C. Vogler, A. Klein, W. Kaim, *Inorg. Chem.* **1996**, *35*, 1295−1300.
[38] A. Klein, C. Vogler, W. Kaim, *Organometallics* **1996**, *15*, 236−244.
[39] M. R. Waterland, K. C. Gordon, J. J. McGarvey, P. M. Jayaweera, *J. Chem. Soc., J. Chem. Soc., Dalton Trans.* **1998**, 609−616.
[40] R. E. Holmlin, J. A. Yao, J. K. Barton, *Inorg. Chem.* **1999**, *38*, 174−189.
[41] R. M. Hartshorn, J. K. Barton, *J. Am. Chem. Soc.* **1992**, *114*, 5919−5925.
[42] H. D. Stoeffler, N. B. Thornton, S. L. Temkin, K. S. Schanze, *J. Am. Chem. Soc.* **1995**, *117*, 7119−7128.
[43] A. Klein, T. Scheiring, W. Kaim, *Z. Anorg. Allg. Chem.* **1999**, *625*, 1177−1180.
[44] W. B. Connick, R. E. Marsh, W. P. Schaefer, H. B. Gray, *Inorg. Chem.* **1997**, *36*, 913−922.
[45] A. Klein, H.-D. Hausen, W. Kaim, *J. Organomet. Chem.* **1992**, *440*, 207−217.
[46] A. Klein, W. Kaim, E. Waldhoer, H.-D. Hausen, *J. Chem. Soc., Perkin Trans. 2* **1995**, 2121−2126.
[47] S. Achar, V. J. Catalano, *Polyhedron* **1997**, *16*, 1555−1561.
[48] A. Klein, J. van Slageren, S. Záliš, *J. Organomet. Chem.* **2001**, *620*, 202−210.
[49] M. Kato, C. Kosuge, S. Yano, M. Kimura, *Acta Crystallogr., Sect. C* **1998**, *54*, 621−623.
[50] R. S. Osborn, D. Rogers, *J. Chem. Soc., Dalton Trans.* **1974**, 1002−1004.
[51] M. Textor, H. R. Oswald, *Z. Anorg. Allg. Chem.* **1974**, *407*, 244−256.
[52] S. Hasenzahl, H.-D. Hausen, W. Kaim, *Chem. Eur. J.* **1995**, *1*, 95−99.
[53] I. R. Farrell, J. van Slageren, S. Záliš, A. Vlček, Jr., *Inorg. Chim. Acta* **2001**, *315*, 44−52.
[54] W. P. Schaefer, W. B. Connick, V. M. Miskowski, H. B. Gray, *Acta Crystallogr., Sect. C* **1992**, *48*, 1776−1778.
[55] J. D. Scott, R. J. Puddephatt, *Organometallics* **1983**, *2*, 1643−1648.
[56] C. Eaborn, K. Kundu, A. Pidcock, *J. Chem. Soc., Dalton Trans.* **1981**, 933−938.
[57] H. C. Clark, L. E. Manzer, *J. Organomet. Chem.* **1973**, *59*, 411−428.

[58] C. Vogler, B. Schwederski, A. Klein, W. Kaim, *J. Organomet. Chem.* **1992**, *436*, 367−378.
[59] G. M. Sheldrick, *SHELXTL-PLUS: An Integrated System for Solving, Refining and Displaying Crystal Structures from Diffraction Data*; Siemens Analytical X-ray Instruments Inc., Madison, WI, **1989**.
[60] G. M. Sheldrick, *SHELXL-97: A program for Crystal Structure Determination*; Universität Göttingen, Göttingen, **1997**.
[61] E. M. Kober, J. L. Marshall, W. J. Dressick, B. P. Sullivan, J. V. Caspar, T. J. Meyer, *Inorg. Chem.* **1985**, *24*, 2755−2763.
[62] C. J. Kleverlaan, D. J. Stufkens, I. P. Clark, M. W. George, H. van Willigen, A. Vlček, Jr., *J. Am. Chem. Soc.* **1998**, *120*, 10871−10879.
[63] C. Fonseca Guerra, J. G. Snijders, G. te Velde, E. J. Baerends, *Theor. Chim. Acta* **1998**, *99*, 391−403.
[64] S. J. A. van Gisbergen, J. G. Snijders, E. J. Baerends, *Comput. Phys. Commun.* **1999**, *118*, 119−138.
[65] M. J. Frisch, G. W. Trucks, H. B. Schlegel, G. E. Scuseria, M. A. Robb, J. R. Cheeseman, V. G. Zakrzewski, J. A. Montgomery, Jr., R. E. Stratmann, J. C. Burant, S. Dapprich, J. M. Millam, A. D. Daniels, K. N. Kudin, M. C. Strain, O. Farkas, J. Tomasi, V. Barone, M. Cossi, R. Cammi, B. Mennucci, C. Pomelli, C. Adamo, S. Clifford, J. Ochterski, G. A. Petersson, P. Y. Ayala, Q. Cui, K. Morokuma, D. K. Malick, A. D. Rabuck, K. Raghavachari, J. B. Foresman, J. Cioslowski, J. V. Ortiz, A. G. Baboul, B. B. Stefanov, G. Liu, A. Liashenko, P. Piskorz, I. Komaromi, R. Gomperts, R. L. Martin, D. J. Fox, T. Keith, M. A. Al-Laham, C. Y. Peng, A. Nanayakkara, C. Gonzalez, M. Challacombe, P. M. W. Gill, B. G. Johnson, W. Chen, M. W. Wong, J. L. Andres, M. Head-Gordon, E. S. Replogle, J. A. Pople, *Gaussian 98 (Revision A.6)*, Gaussian, Inc., Pittsburgh, PA, **1998**.
[66] A. D. Becke, *Phys. Rev. A* **1988**, *38*, 3098−3100.
[67] J. P. Perdew, *Phys. Rev. B* **1986**, *33*, 8822−8824.
[68] E. van Lenthe, A. Ehlers, E. J. Baerends, *J. Chem. Phys.* **1999**, *110*, 8943−8953.
[69] D. E. Woon, T. H. J. Dunning, *J. Chem. Phys.* **1993**, *98*, 1358−1371.
[70] D. Andrae, U. Haeussermann, M. Dolg, H. Stoll, H. Preuss, *Theor. Chim. Acta* **1990**, *77*, 123−141.
[71] P. J. Stephens, F. J. Devlin, C. F. Cabalowski, M. J. Frisch, *J. Phys. Chem.* **1994**, *98*, 11623−11627.

Received November 8, 2002

